Bachelor Thesis

Development and comparison of open- and closed-loop control of untethered microrobots in a tuneable magnetic trap

Robert van de Weerd

Graduation committee
Prof. dr. Sarthak Misra
Dr. Franco P. Basualdo
Dr. ir. Arvid Keemink

August 29, 2023

B-939
Department of Biomedical Engineering

UNIVERSITY OF TWENTE.

SURGICAL ROBOTICS LABORATORY

Contents

1 Introduction

Magnetic actuation of microparticles has several potential application in bio medicine. For example, the control of microrobots in the human body allows for local and selective engagement of human cells and tissue. [1] This gives possibilities for minimally invasive surgeries, in many regions of the body including abdomen, heart, brain, eye, ear and vascular system. [2] Microrobots can be used for delivering of therapeutic substances via the bloodstream, micromanipulation of cells and development of new drugs. [3] [4]

Through the research of driving and controlling microrobots, it is found that energy supply is the most challenging part. Energy supply of microrobots can be divided in chemical drive and physical drive. Physical drive mainly uses electric field, magnetic field light field and sound field. [5] In this research physical drive by magnetic field will be investigated. This concept of generating force on a microrobot by magnetism has been considered as a promising technique.

In the current-state-of-art, different methods are investigated to actuate the microrobot. One of the methods is the trapping and actuation of the microrobot by gradient pulling using the OctoMag system. [2] [6] A set of 8 external electromagnets, that can surround a human head, provide a magnetic field in a 3D workspace with a diameter of 25 mm. One of the disadvantages of this system is the large distance between the coils and the electromagnets, which makes it difficult to create high magnetic field gradients, so creating high magnetic forces is a challenge.

A second method is a device called Microrobotic Infrastructure Loaded into Magnetically-Actuated Catheter (MILiMAC). This device uses three miniaturized electromagnets, which can be delivered to a microsurgery site and be deployed, creating a two-dimensional workspace. [3] However, this miniaturized coils can create only small amount of magnetic force without getting heated, what limits the opportunities of this method.

A third method is the insertion of three needle-shaped electromagnets around the target site. [7] With that, a compact 2D workspace can be created where the particle is trapped and can be actuated. The biggest disadvantage of this system is the creation of heat inside the human body, what limits the magnitude of the magnetic field that can be used.

In this work a system is investigated that uses external coils for creating a magnetic field, and 3 local ferrite rods for creating the field gradient. With this system, large magnetic fields are created without heating of the human tissue, and large gradients and forces are created using local actuation of the microrobot by magnetized ferrite rods. For this system image-based control of the microrobot is investigated. To enable this, image analysis is used for tracking of the microrobot. An open loop and closed loop control system are created, tested and compared.

2 Magnetic actuation

The microrobot will be moved by magnetic actuation. This actuation is enabled by magnetic gradient forces. This forces, that make the robot move, arise from a gradient in a magnetic field called ∇B, with unit T/m. This means that the magnetic field is not the same at every location in the workspace, but changes over distance. This force is given by this function where m is the magnetic dipole moment and B is the magnetic field:

$$F = \nabla(m \cdot B) \tag{1}$$

This equation shows that the magnetic force is larger when the gradient of the magnetic field is larger.

In this work, we develop control algorithms for the manipulation of particles in a tunable magnetic trap. In a magnetic trap, a magnetic particle is trapped my magnetic forces. This means, the particle is held in place by the magnetic forces. A tunable magnetic trap means that the magnetic forces, that hold the particle in place, can be enlarged and reduced. Varying of the magnetic forces is enabled by changing the magnetic field magnitude B, as shown in equation 1. In this work, the magnetic trap actuation system consists of two main components: A Helmholtz coils system for magnetic field generation, and ferrite rods for the generation of magnetic gradients. This trap can control magnetic particles using the applied external magnetic field as control signal.

2.1 Helmholtz coils

The Pacmag system exists of three pairs of Helmholtz coils placed orthogonally, as shown in Figure 1. With this set of coils a magnetic field can be created in all directions in 3D space.

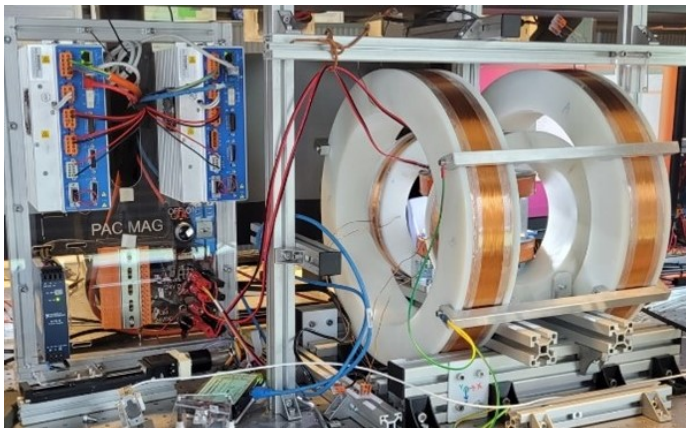

Figure 1: The PacMag system at Surgical Robotics Lab. [8]

A pair of Helmholtz coils consists of two air-core electromagnets on the same axis where an equal current flows in the same direction.[9] Between these electromagnets a nearly homogeneous magnetic field is created. The magnitude of this magnetic field can be regulated by changing the current through the electromagnets. (Figure 2) The current in each coil pair is controlled by Xenus XE2-230-20 amplifiers (Copley Controls, Canton, USA).

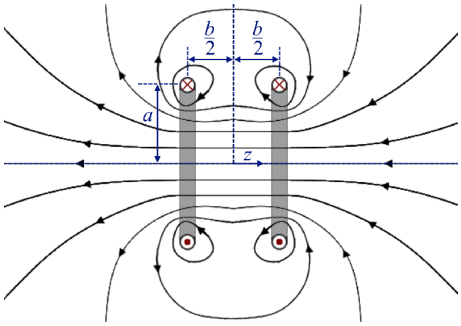

Figure 2: schematic representation of a pair of Helmholtz coils, showing a nearly homogeneous field between the coils. [9]

2.2 Ferrite rods

In the PacMag system, the generated magnetic field is almost homogeneous. A homogeneous magnetic field means that the magnetic forces are negligible. We use ferrite rods to generate magnetic field gradients. A ferrite rod is made of magnetic material with a relative permeability of >2000, and in this work they have a length of 15 mm and a diameter of 2 mm. In a homogeneous field, the magnetic field lines are straight. (Figure 3) If a ferrite rod is placed in a magnetic field, it will be magnetized and locally concentrate the field lines.[10] However, given the elongated shape of the rod, its magnetization depends on the relative orientation between the magnetic field and the rod. (Figure 3) With that a magnetic trap is created around the ends of the rod, where the magnetic field is concentrated. From physical principle can be stated that a magnetized particle is attracted to a location with the strongest magnetic field (highest density of magnetic lines). [11] From this can be concluded that the micro particle is attracted to the ferrite rod when the magnetic field is in line with the ferrite rod.

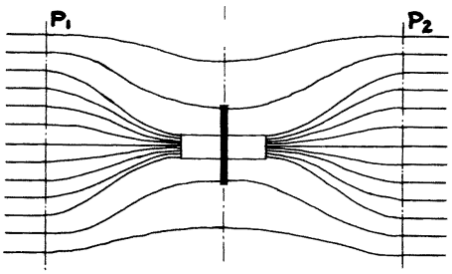

Figure 3: Magnetic field change by ferrite rods. [10]

In this work 3 ferrite rods are used to create a 2D tunable magnetic trap capable of exerting forces in any direction in 2D plane. A plastic mould is created where the ferrite rods are attached to, and the particle is placed in the middle as shown in figure 4.

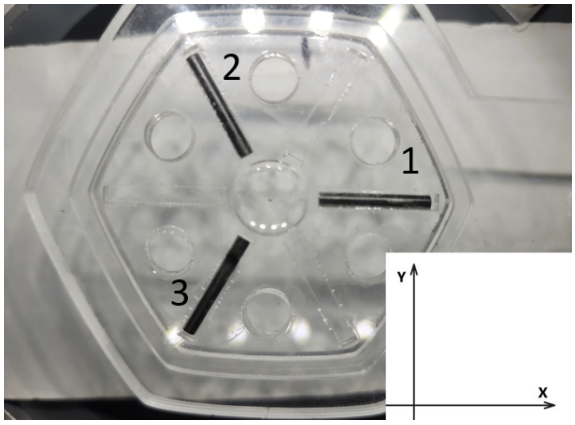

Figure 4: Ferrite rods system

A ferrite rod creates the strongest magnetic attraction on the particle when the magnetic field is in line with the ferrite rod. For example, when the magnetic field is created in x direction ferrite rod number 1 is magnetized more than the others, as shown in figure 5a. The magnetic particle placed between the rods will be more attracted by rod 1, making the particle move to the right. To let the particle move to the left, ferrite rods 2 and 3 must be equally magnetized and stronger than ferrite rod 1. This can be done by creating a field in y direction as shown in figure 5b. Since the system is symmetric, the same analysis can be made for the remaining rods.

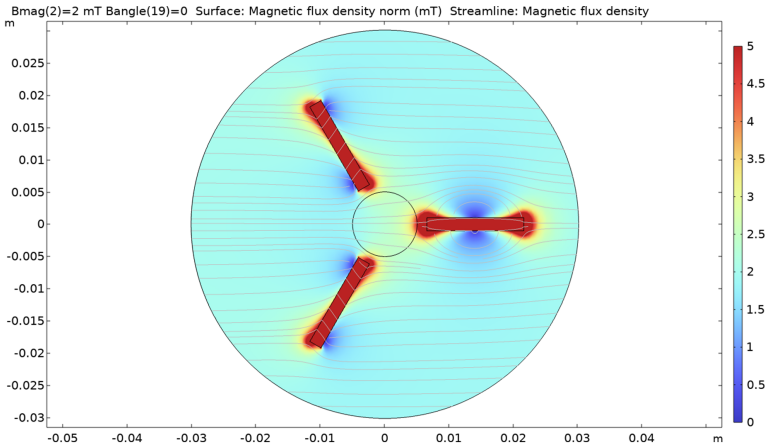

(a) Ferrite rods magnetization for magnetic field angle is 0 deg.

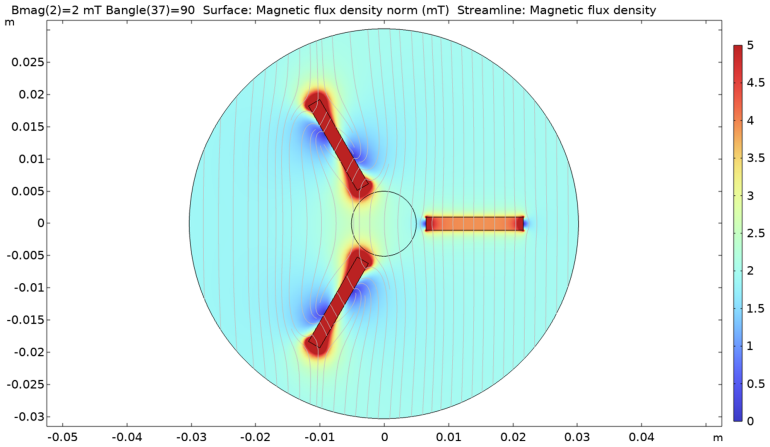

(b) Ferrite rods magnetization for magnetic field angle is 90 deg.

Figure 5: Magnetization of ferrite rods, for magnetic field angles 0 and 90 degrees.

2.3 Actuating the microparticle

In this research a 0.5 mm steel sphere, made of stainless steel AISI 420C, represents the microrobot. This particle is soft magnetic, which means that the particle does not retain its magnetization when there is no external field. It needs to be magnetized by an external field. Soft magnetic means that the particle is easily magnetized and has a low coercivity. [12] The magnetic dipole moment m of a soft magnetic particle is given this function where K_m is the magnetization constant:

$$m = k_m * B \tag{2}$$

When we substitute equation 2 into the magnetic force equation 1, we find that the magnetic force on a soft magnetic particle is given by

$$F_{mag} = K_m \nabla |B|^2 \tag{3}$$

To avoid friction and adhesion problems with a solid substrate, the microparticle is floating on a small amount of water. Water was chosen because of its low viscosity, enabling fast motion of the particle, and because of the high surface tension, enabling the particle to float at the interface. However, water will evaporate a lot faster than other fluids like oil, but with these more viscous fluids the movement of the particle will be very slow. This water forms a curved meniscus, which gives place to capillary forces pulling the particle to the center, as shown in figure 6.

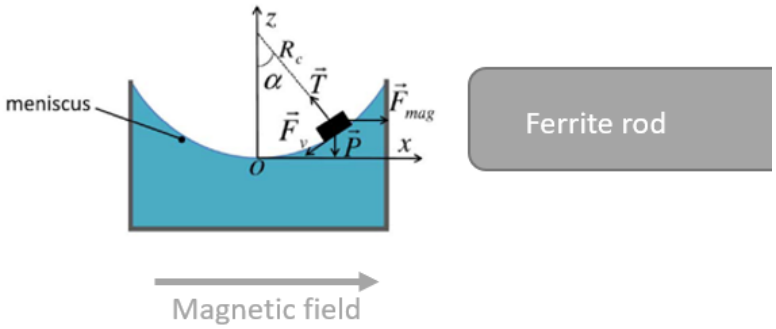

Figure 6: schematic view of the water meniscus and one of the ferrite rods.

The force that is needed to move the particle to a higher position in this meniscus can be calculated by the following formula: [13]

$$F_{cap} = \frac{m * g}{R_c} * \bar{x} \tag{4}$$

In this function m is the mass of the particle, g is the gravitation constant, R_c is the meniscus curvature and x is the distance from the center. However, the setup used in this research can be subject to inhomogeneities due to contact angle hysteresis. Contact angle hysteresis means that the particle can stick to the fluid even when the fluid is at an certain angle, so there is a certain minimum angle before the gravity force will win. [14] This induces variability in the shape of the meniscus, that results in changes of the force that is needed to move the particle. Therefore, the relationship between magnetic field magnitude and the displacement of the particle will be calculated by carrying out experimental characterisations. By exciting a certain magnetic field magnitude, there can be determined what displacement the particle experiences. That relation can be used other way around, to calculate the desired magnetic field. This is further described in section 3.

3 Control systems

This assignment aims on controlling the soft magnetic particle with a closed loop control system. This aim is divided into several tasks. Firstly the location of the particle must be tracked by image analysis. After doing this, the system must be characterized. From this characterisation, an open-loop and closed-loop control system can be developed.

3.1 Tracking

To make it possible to create a closed-loop control system and to characterize the system, the location of the particle must be tracked. This is done by using a camera that is placed above the workspace. Image analysis with openCV is used to detect the location of the particle.

Several steps are involved to make this possible. First the image from the camera is blurred, cropped and changed to grayscale image. After that a binary image is created. from this binary image the contours of the particle can be easily detected by using 'findContours'. The output of this function is 2D function. This steps are shown in figure 7. After this an image moment is calculated from this function, that is defined as:

$$M_{pq} = \iint_{-\infty}^{\infty} x^p y^q f(x,y) dx dy \tag{5}$$

This image moment is a weighted average of the pixel intensities in the function. The center of an image moment can be calculated as follows:

$$x, y = \frac{M_{10}}{M_{00}}, \frac{M_{01}}{M_{00}} \tag{6}$$

In this function, M_{00} is the area of the image, where p and q are zero. M_{10} is used to calculate the x component of the center point, where p=1 and q=0. M_{01} is used to calculate the y component of the center point, where p=0 and q=1.

Using this contours the midpoint of the particle can be determined, and expressed in pixels. For a known position of the particle, and known pixel size, the location of the particle can be calculated in mm.

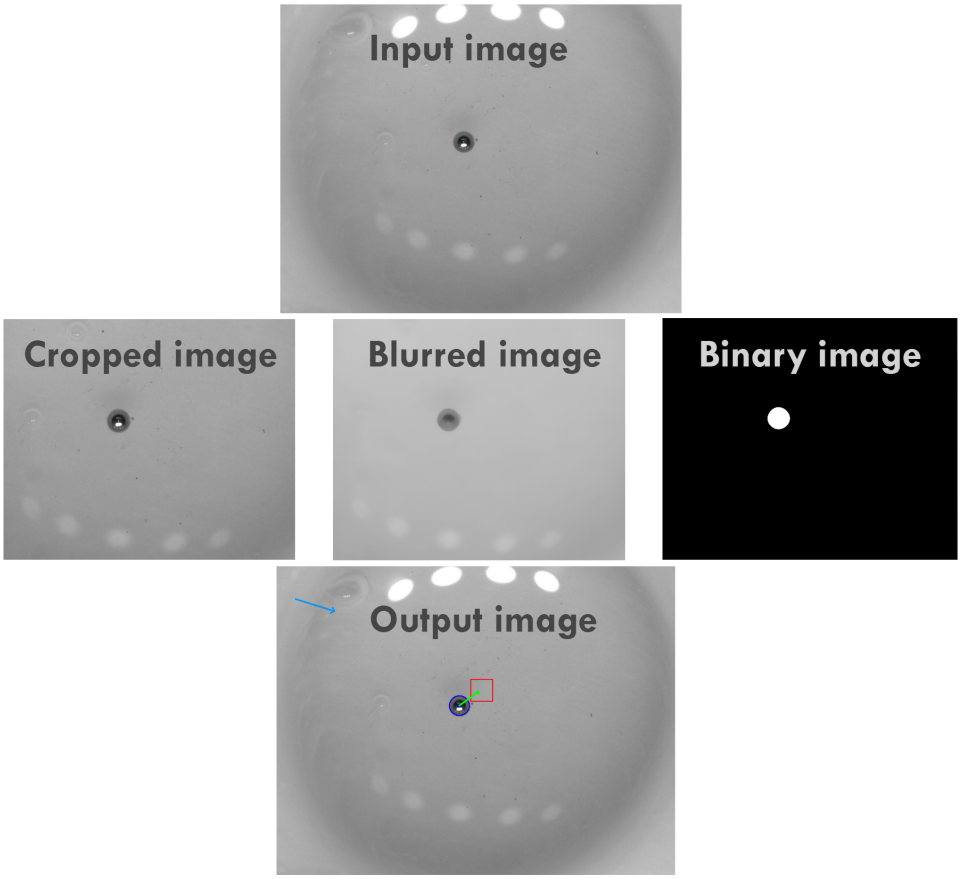

Figure 7: The steps that are involved for tracking the particle location.

The image tracking by openCV is implemented in C++ as shown in appendix A.1.

3.2 Characterisations

The system has to be characterized to define the relationship between magnetic field and movement of the particle. To characterise the system a steady and dynamic characterisation are carried out. With steady characterisation we can determine the magnetic field required to reach a certain position.

The steady characterisation is carried out by moving the particle helix-wise as shown in Figure 8b. This helix movement is created by increasing the field 0.025 mT/s, and slowly rotating with a speed of 54 deg/s. The applied magnetic field during this characterisation is shown in Figure 8a.

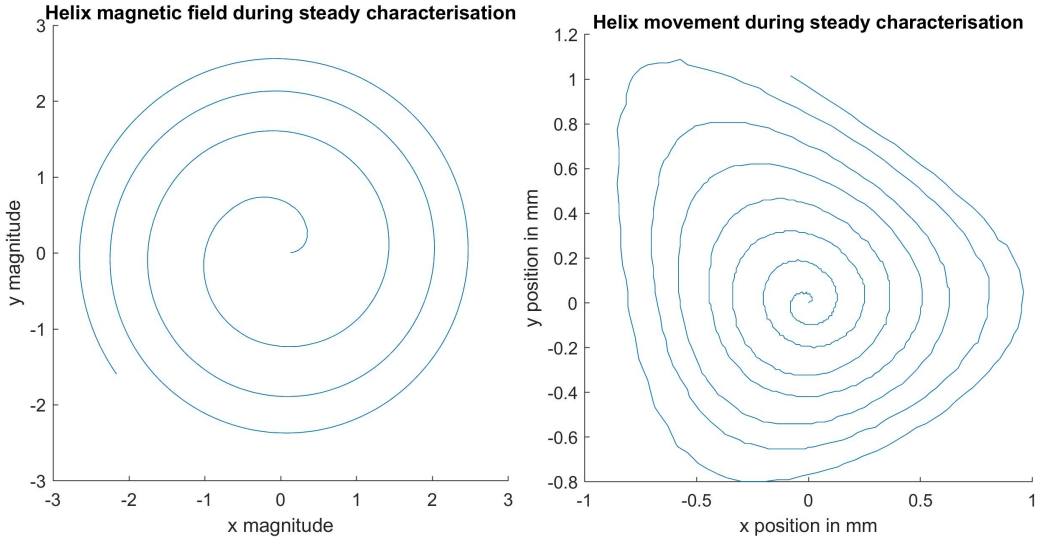

(a) The applied magnetic field during steady characterisation

(b) movement of the particle during steady characterisation

From this characterisation a figure is created where the magnetic field magnitude B is plotted against the distance from the center, as shown in figure 9a.

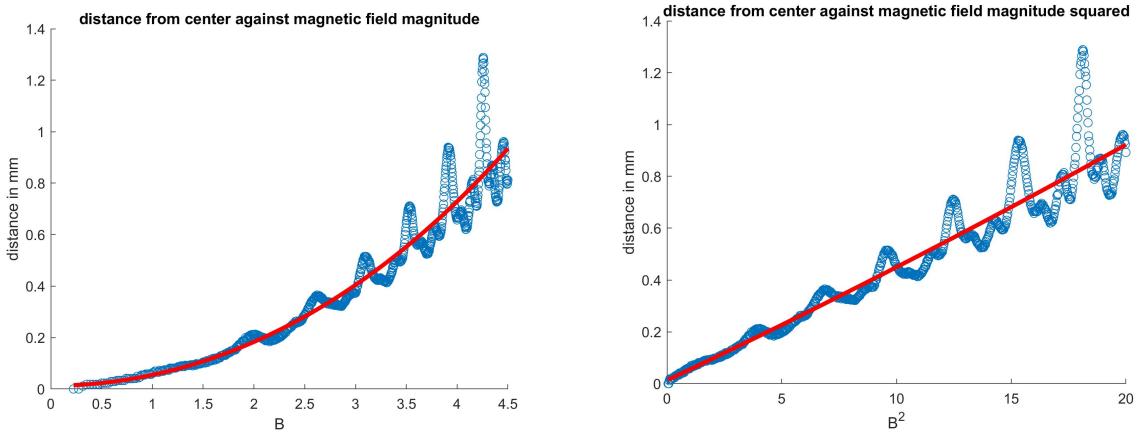

(a) B

(b) B^2

Figure 9: Magnetic field magnitude against distance from origin

From this characterisation can be stated that the maximum applied field is around 5 mT. With a larger magnetic field, the particle became unstable and jumped to the edge of the plastic mould. The relationship between the magnetic field magnitude and the distance is quadratic. This can be proved by plotting the magnetic field squared (B^2) against the distance from the center as shown in figure 9b. Figure 9b shows a linear relationship between distance and B^2, as shown in equation 7, where x is the distance from the center. The factor K can be determined from figure 9b and is estimated as K=1/21.6 mm/mT^2.

$$\overline{x} = K * |\overline{B}|^2 \tag{7}$$

On the other hand the magnetic field angle can be characterized. To do that, the magnetic field angle is plotted against the position angle of the particle. The result of this characterisation is shown in figure 10.

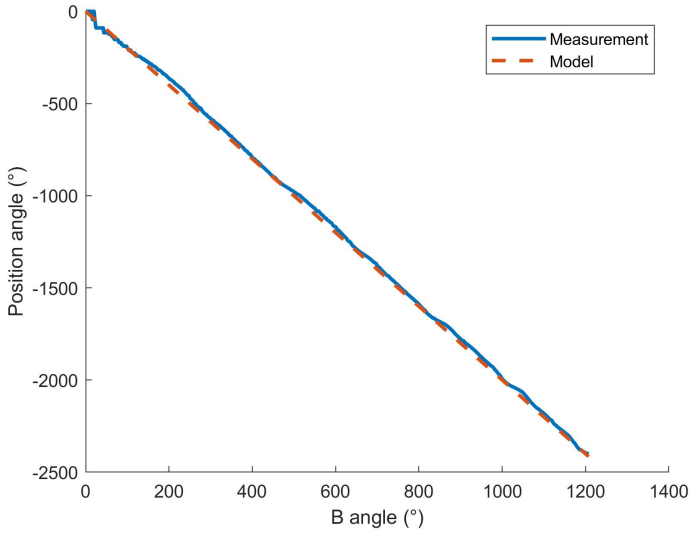

Figure 10: The magnetic field angle and particle position angle during steady characterisation.

From this figure can be concluded that the relationship between magnetic field angle and resulting magnetic force is given by the following equation:

$$\theta_u = -2\theta_B \tag{8}$$

This corresponds with figure 5.

For the dynamic characterisation a step function in the magnetic field is created for time = 5 seconds. This is carried out for values of 3 mT and 5 mT. The result is shown in figure 11.

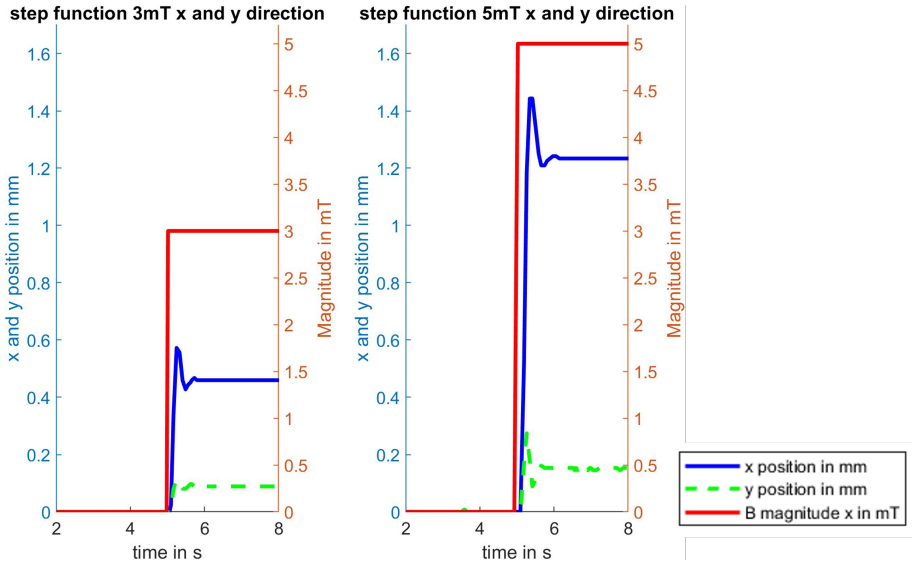

Figure 11: Magnetic field magnitude and position, during the dynamic characterisation

With this characterisation the overshoot and settling time can be determined. The overshoot is calculated by measuring the stable position of the particle, and the highest point of the overshoot peak. The actual overshoot is the difference between these two. It can be expressed as a percentage of the stable position. It turns out to be 25 % for 3 mT and 15% for 5mT. The settling time can be determined by calculating the time difference between the time of the step function (t=5s) and the moment the particle does not move anymore. There can be calculated that the setting time is around 1s for 3 mT and 1.2s for 5 mT.

3.3 System model identification

Using this characterisations the physical system can be modelled. The characterisations give information about the reaction of the system on a certain input. So, a model of the system can be created, that gives the output of the system for a given input. To relate the output to the input, the following input-output relation in time domain is given:

$$x(t) = \mathbf{G}u(t) \tag{9}$$

This equation gives the relation between the input u and the output x of the system **G**. From the characterisations, we know that the applied force relationship to the magnetic field is non-linear. Therefore, we define the control variable u as

$$\begin{cases} |\overline{u}| = \quad |\overline{B}|^2 \\ \theta_u = -2 * \theta_B \end{cases} \tag{10}$$

which linearly related to the applied force. The system has to create a magnetic force that counteracts the capillary force of the meniscus and the drag force of the friction between the particle and the water surface. This means that F_{mag} has to be equal to $F_{cap} + F_{drag}$. These 3 forces are given by the following equations:

$$\begin{cases} F_{mag} = K\overline{u} \\ F_{cap} = \frac{mg}{R_c}\overline{x} \\ F_{drag} = b_d\dot{\overline{x}} \end{cases} \tag{11}$$

In the first equation K is the relation between the system input u and the magnetic force F_{mag}. This factor K is determined by steady characterisation. In the second equation m is the mass of the particle, g is the gravitation constant, R_c is the meniscus curvature and x is the distance from the center. In the third equation b_d is the drag force constant.

Using Newtons second law results in the following equation:

$$m\ddot{\overline{x}} = K\overline{u} - \frac{mg}{R_c}\overline{x} - b_d\dot{\overline{x}} \tag{12}$$

Rewriting this equation, and transforming into Laplace domain, we get the following transfer function:

$$\overline{x} = \frac{K}{ms^2 + b_d s + \frac{mg}{R_c}}\overline{u} \tag{13}$$

which is a second-order transfer function. However, the values of R_c an b_d are unknown. Therefore, we use the dynamic characterisation results to estimate the damping and natural frequency of the system. This can be done by using the standard second order transfer function with real parameters ω_n and ζ.

$$G(s) = \frac{output}{input} = \frac{x(s)}{u(s)} = \frac{\omega_n^2}{s^2 + 2\zeta\omega_n s + \omega_n^2} \tag{14}$$

Using the measured values of the step response, like settling time and overshoot, a model identification can be done to determine the values for ω_n and ζ. For this, the MatLab app 'System Identification' is used. By inserting the above determined values we get ω_n = 7.8 Hz and ζ = 0.38.

3.4 Open-loop control system

With the results of this characterisations an open-loop control system can be created. From the steady characterisation we derived factor K, that relates the desired magnetic field magnitude for a position of the particle in mm. This factor K depends on F_{cap} and F_{drag}, as we conclude from equation 13. When one of these forces increases, K must increase to have the correct counteracting force F_{mag}. Also, the relation between magnetic field angle and required force angle is investigated. This means that a feed forward control system can be created by using this values. This is shown in the following set of equations:

$$\begin{cases} |B| = -\sqrt{(|u|)} \\ \theta_B = \quad -\frac{1}{2}\theta_u \end{cases} \tag{15}$$

To have the right input for the PacMag system, the magnetic field is seperated in an x and y component as follows:

$$\begin{aligned} Xfield &= |B| * cos(\theta_B) \\ Yfield &= |B| * sin(\theta_B) \end{aligned} \tag{16}$$

This output is given in mT. The required currents, that are send to the coils, are calculated based on a previously performed calibration of the system.

The performance of this open loop control system can be evaluated numerically by carrying out a dynamic characterisation. To do this, a desired position of [0.5, 0.5] is given at time = 5s. The result is shown in figure 12.

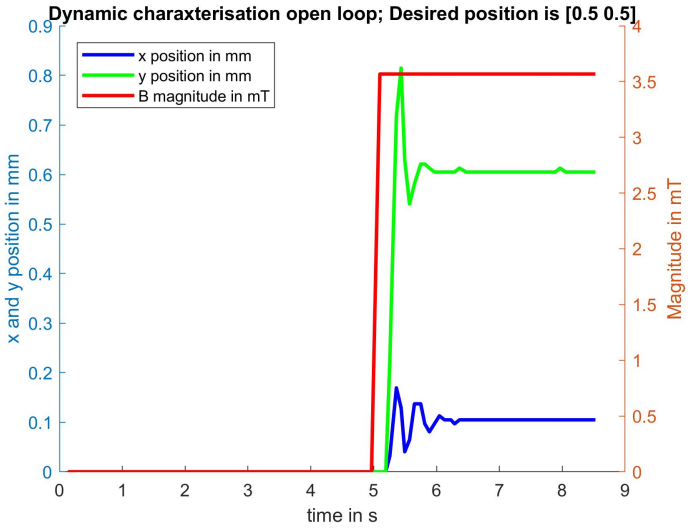

Figure 12: Dynamic characterisation for desired position [0.5, 0.5] with an open-loop control system.

This figure shows that the open-loop control system has a large steady-state error. In this situation, the steady-state error for x is around 0.4 mm, and for y around 0.1 mm. However, this steady state error differs for each location of the particle. From figure 13 can be seen that the steady-state error is not that large for every location.

The settling time for the x position is around 1.1s and the percentage overshoot (%OS) is around 62%. For y position, the setting time is around 1s, and the %OS is around 34%.

With this a control system a square can be drawn as shown in figure 13. To do this, te particle is send to locations [-0.5,0.5], [0.5,0.5], [0.5,-0.5] and [-0.5,-0.5] successively. In this figure, a red block is drawn for the desired location of the particle. From the center of the particle green arrow is drawn, that shows the current desired movement direction and force.

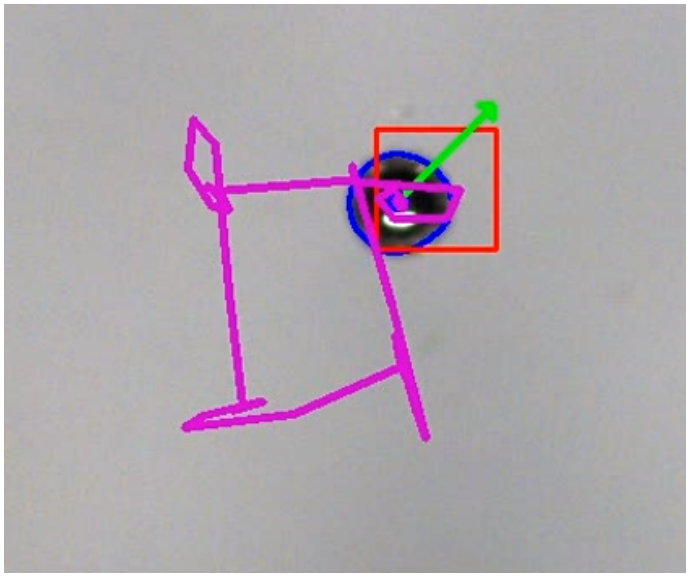

Figure 13: Draw a square with closed-loop control system

To test the usability of the system, we tried to write SRL, by moving the particle using mouseclicks. This is done by creating a script that detects mouse clicks on the image, and calculates a desired position for the particle. By clicking many times, the letters SRL can be written manually. The implementation of this in c++ can be found in appendix A.5. During this drawing the user actively corrected for the steady state error. This result is shown in figure 14.

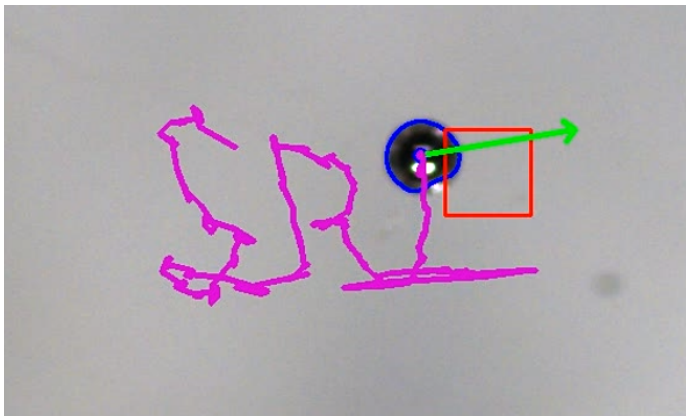

Figure 14: Writing SRL with open-loop control system

From above results we state that the open-loop control system is a fast method to control the micro-robot, with a low settling time. However the large steady state error makes this system almost unusable for further applications. Thereby, an overshoot of 62 % for x position is definitely too large to make this system a usable control system. To solve this problems, the use of a closed-loop control system is investigated.

3.5 Closed-loop control system

By using feedback from the camera a closed-loop control system can be created. This can be done by calculating the error between the current and desired position and using a PID-controller. The derivative part of this PID-controller was not used, because of the lack of a good estimation of the particles velocity. The visual feedback algorithm that has been developed provides the particle position in whole pixels, meaning that the position may vary plus/minus one pixel each time step, what results in a large noise

if the velocity is estimated by traditional Finite Difference. Therefore a PI controller is used, where the desired magnetic force is calculated as follows:

$$\overline{u} = K_p * error + \int K_i * error\, dt \tag{17}$$

K_p and K_i are the gains that are used to tune the PI-controller. The x and y error are calculated separately, so control is also separated in an x and y part. The error is determined by subtracting the current location, based in image analysis, from the desired location. The implementation of the PI-controller in C++ is shown in appendix A.3.

From the system identification the values for ζ, ω and K were found. This system identification can be inserted in the "PID Tuning" app in Matlab. This PID tuning gives the following values: $K_p = 0.5mT^2/mm$ and $K_i = 15mT^2s/mm$.

For this values, a dynamic characterisation is carried out. To do that, a desired position [0.5 0.5] is given at time = 5s. With that characterisation the overshoot and settling time can be determined. The results are shown in Figure 15.

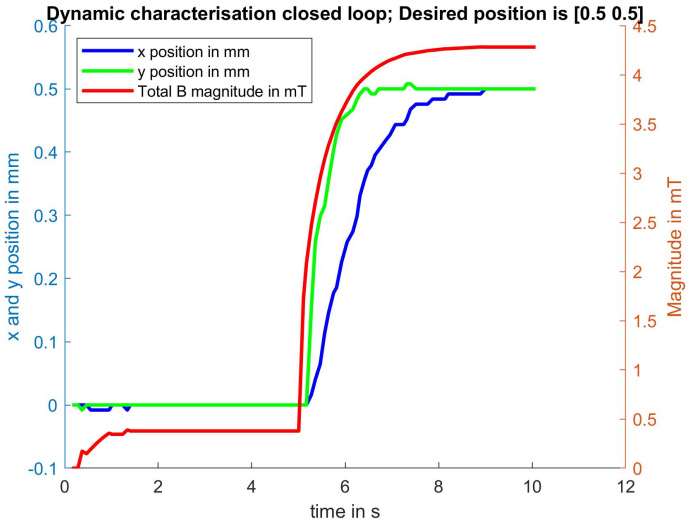

Figure 15: Dynamic characterisation for desired position [0.5 0.5]. Carried out for $K_p = 0.5mT^2/mm$ and $K_i = 15T^2s/mm$.

From this characterisation the settling time and overshoot can be determined. From the figure can be concluded that the overshoot is negligible. The settling time is around 1.7 seconds for the y position, and around 4 seconds for the x position. The steady-state error is also negligible. The total magnetic field magnitude is around 4.3 mT in this experiment.

After this characterisation, a script is created to draw a square of 1 by 1 mm. To create a repeatable experiment, desired location points are given by the script. Mouseclick is not used for this experiment. This result is shown in Figure 16. In this experiment a line is drawn at the location the particle has been. In this way a square can be clearly drawn.

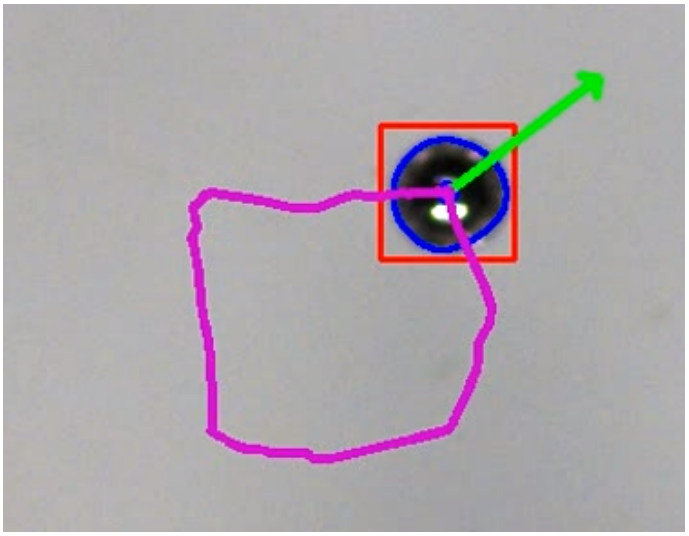

Figure 16: Draw a square with closed-loop control system.

Finally, the usability of this control system is tested again by writing the letters SRL, using mouseclicks. This result is shown in figure 17.

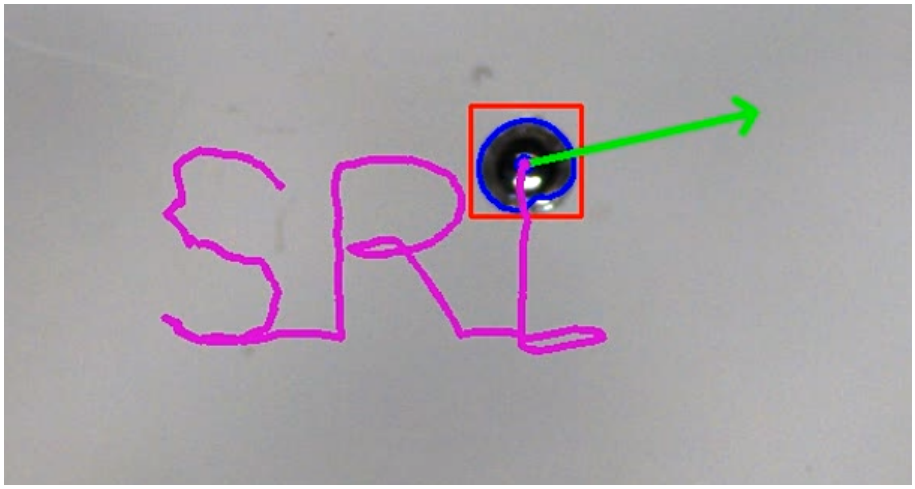

Figure 17: Writing SRL with closed-loop control system

We can conclude from this results that the closed-loop control is a precise method to control the microrobot. The steady state error is negligible what enables the possibility to write SRL nicely. The lack of overshoot also makes this system a better one than the closed-loop system.

4 Discussion

This assignment aimed on controlling a microrobot in a tunable magnetic trap. This magnetic trap is made using a set of Helmholtz coils and a ferrite rods system.

This contains research on the used magnetic trap system, and investigate the advantages. This system also has to be characterized, by system identification. It also encloses tracking the particle using image analysis. After that a open-loop and closed-loop control system are developed to control the particle. This control systems are evaluated and have been compared.

The first problem that was encountered during the research is the instability of the meniscus of water. The water was leaking out of the plastic workspace, which results in a decrease of amount of water over time. So the shape of the meniscus became steeper after a certain amount of time. This makes it almost impossible to perform a steady characterisation, and use the calculated value for the open-loop control. Therefore the K value was corrected while performing the experiments. For example, while drawing SRL with open-loop control a K-value of 1/18 mm/mT^2 was used, while the calculated value from the characterisations was 1/21.6 mm/mT^2. To solve this problem a closed-loop control system was investigated. The use of a feedback loop automatically compensates for this instability.

The inhomogeneity of the magnetic field causes unexpected movements of the particle. From figure 8b we see that the movement of the particle is not a helix although it was controlled to do that. The field inhomogeneity also causes an instability of the particle when the applied magnetic field is around 6 mT or higher. This results in a relative small workspace of only 2x2 mm. This is a lot smaller than the workspace of the octomag system, investigated by Ebrahimi et al [2]. This system uses external coils to create magnetic field and field gradient, what results in a workspace of 25 mm. However, the created magnetic field gradient is only 0.35 T/m, while our system can in principle create gradients up to 5 T/m. Also the workspace of the MiliMac system, researched by Sikorski et al [3], is a lot bigger, having a triangular workspace with sides of 16 mm. However, The MiliMac system was not stable at every location in the workspace.

For surgical applications heating effects are undesirable and can be hazardous. The use of external coils results in a lack of heating effects in the human body. The dissipated power of the Milimac system [3] is around 0.96 W. For the Magneed system, researched by Huaroto et al [7], the power consumption is around 0.5 W. Both of these systems use the technique of internal field creation, in the human body. Our system, using the external helmholtz coils to create the field, results in negligible heating in the human body, what has positive effects on the safety of the system.

5 Future work

The system is limited by the instability of the particle when it has a certain distance from the center. Better design of the Helmholtz coils, ferrite rods and other parts of the system can possibly lead to an increase of the workspace. This will also decrease deviations in the magnetic field. This will result in higher predictability of the system and a lower steady state error for open-loop control.

The tuning of the PI-controller using model-predictive techniques can be performed better. With that, the performance of the control system will increase. For example, it must be possible to lower the settling-time by increasing the gains.

Also, the derivative part of the PID controller can be added, only if a solution is found for a velocity estimation without large noise. This can be done by implementing a state observer that estimates the system complete state.

The designed control system can be used for a wide range of applications. Controlling of microrobots can have a future in minimally invasive surgery or micromanipulations of cells.

This type of control system can be applied for different solutions and equipment. The use of different camera's, for example MRI imaging in a human body, should be possible. The tracking of the particle is theoretically possible for every type of imaging. Also the actuation can be designed differently, for applications in medical context.

6 Conclusion

The steps carried out in this research lead to a number of interesting conclusions.

This research shows that it is possible to control a microrobot by using external Helmholtz coils and local ferrite rods. With this method, relative high magnetic fields can be used (up to 50 mT), compared to the use of local miniaturized electromagnets (<10 mT). The created magnetic field gradient by the ferrite rods is relatively high (5 T/m), compared to the use of external coils (only 1 T/m). This enables the precise control of the particle with fields of only 5 mT.

Tracking of the particle by a camera using image-analysis worked out as a good solution to provide image-based control of the microrobot. The detection of the particle location worked properly without problems.

System identification gives good insight in the properties of the system. When the characteristic values of the system are known, like damping ratio and natural frequency, tuning of the PI controller is done reliable and easy.

With the designed open-loop control system the particle could be moved in desired direction. However, the exact position is never reached. Deviations in the field are making it almost impossible to calculate a correct magnitude and direction for every location in the workspace.

To solve this a closed-loop control system was designed, which can handle deviations in the system. A closed-loop control system uses feedback from the camera to determine the desired magnetic field. The magnetic field is depending on the error between desired and current position, and in this way deviations are canceled out easily.

The results of both methods show that the closed-loop control system is better in reaching the desired location. The steady-state error after stabilization of the particle is negligible for closed-loop, while the open-loop system has a relative large steady state error, of almost 0.5 mm. Mainly this problem causes that it was almost impossible to write SRL with the open-loop control system.

The overshoot is a lot bigger for open-loop, than for closed-loop. For open-loop an overshoot of 62 % is measured. In contrast, the overshoot for closed-loop is lower than the tracking resolution. With a closed-loop control system the magnetic field is increased and decreased smoothly. Against that, an open-loop system excites a certain field magnitude at one moment.

The settling time for closed-loop is concluded to be a lot longer than for open-loop. For the dynamic characterisation with closed-loop control and a magnetic field magnitude of 4.3 mT, the settling time is around 4 seconds. For the dynamic characterisation with open-loop control and a magnetic field magnitude of 5 mT the settling time is around 1.2 seconds.

From the experiments can be concluded that the reachable workspace, without the particle becoming unstable, is around 2x2 mm. So when the distance from the center is more than 1 mm, there is a big change the particle is going to become unstable and jump to the edge of the plastic mould. The maximum magnetic field magnitude that can be applied without becoming unstable is around 5 mT.

References

[1] B. J. Nelson, I. K. Kaliakatsos, and J. J. Abbott, "Microrobots for minimally invasive medicine," *Annual Review of Biomedical Engineering*, vol. 12, no. 1, p. 55–85, 2010.

[2] N. Ebrahimi and et al, "Magnetic actuation methods in bio/soft robotics," *Advanced functional materials*, vol. 31, no. 11, 2020.

[3] J. Sikorski, S. Mohanty, and S. Misra, "Milimac: Flexible catheter with miniaturized electromagnets as a small-footprint system for microrobotic tasks," *IEEE Robotics and Automation Letters*, vol. 5, no. 4, pp. 5260–5267, 2020.

[4] C. Chautems, B. Zeydan, S. Charreyron, G. Chatzipirpiridis, S. Pané, and B. J. Nelson, "Magnetically powered microrobots: a medical revolution underway?," *European Journal of Cardio-Thoracic Surgery*, vol. 51, pp. 405–407, 02 2017.

[5] H. Shen, S. Cai, Z. Wang, Z. Ge, and W. Yang, "Magnetically driven microrobots: Recent progress and future development," *Materials and Design*, vol. 227, p. 111735, 2023.

[6] M. Kummer, J. Abbott, B. Kratochvil, R. Borer, A. Sengül, and B. Nelson, "Octomag: An electromagnetic system for 5-dof wireless micromanipulation," *IEEE Transactions on Robotics*, vol. 26, pp. 1006–1017, 05 2010.

[7] J. J. Huaroto, M. Richter, M. Malafaia, J. Kim, C.-S. Kim, J.-O. Park, J. Sikorski, and S. Misra, "Magneed – needle-shaped electromagnets for localized actuation within compact workspaces," *IEEE Robotics and Automation Letters*, vol. 8, no. 6, pp. 3908–3915, 2023.

[8] T. L. Thomas, J. Sikorski, G. K. Ananthasuresh, V. K. Venkiteswaran, and S. Misra, "Design, sensing, and control of a magnetic compliant continuum manipulator," *IEEE Transactions on Medical Robotics and Bionics*, vol. 4, no. 4, pp. 910–921, 2022.

[9] S. Trout, "Use of helmholtz coils for magnetic measurements," *IEEE Transactions on Magnetics*, vol. 24, no. 4, pp. 2108–2111, 1988.

[10] H. J. Laurent and C. A. B. Carvalho, "Ferrite antennas for a.m. broadcast receivers," *IRE Transactions on Broadcast and Television Receivers*, vol. BTR-8, no. 2, pp. 50–59, 1962.

[11] D. E. Pritchard, "Cooling neutral atoms in a magnetic trap for precision spectroscopy," *Phys. Rev. Lett.*, vol. 51, pp. 1336–1339, Oct 1983.

[12] J. J. Abbott, E. Diller, and A. J. Petruska, "Magnetic methods in robotics," *Annual Review of Control, Robotics, and Autonomous Systems*, vol. 3, no. 1, pp. 57–90, 2020.

[13] M. Dkhil, M. Kharboutly, A. Bolopion, S. Régnier, and M. Gauthier, "Closed-loop control of a magnetic particle at the air–liquid interface," *IEEE Transactions on Automation Science and Engineering*, vol. 14, no. 3, pp. 1387–1399, 2015.

[14] L. Gao and T. J. McCarthy, "Contact angle hysteresis explained," *Langmuir*, vol. 22, no. 14, pp. 6234–6237, 2006.

A Appendix

A.1 Image analysis

```
// image analysis
        // Create cropped image;
        Mat cropped_frame = frame(Range(150,850), Range(250,1100));

        // Create gray image;
        Mat gray_image;
        cvtColor(cropped_frame, gray_image, COLOR_BGR2GRAY);

        // Create blurred image;
        Mat blurred_image;
        medianBlur(gray_image, blurred_image, 25);

        //Create binary image;
        Mat binary_image;
        threshold(blurred_image, binary_image, 120, 255,THRESH_BINARY_INV);

        // Draw contours;
        vector<vector<Point> > contours;
        findContours( binary_image, contours, RETR_EXTERNAL,
                                CHAIN_APPROX_SIMPLE, Point(250,150));

        for( size_t i = 0; i< contours.size(); i++ )
        {
            Scalar color = Scalar( 255, 0, 0 );
            drawContours(frame, contours, (int)i, color, 2, LINE_8);
        }
        \
        if (contours.size()==0){
            cout << " Error: No particle detected." <<endl;
            return 1;
        }

        Moments M = moments(contours[0]);

        // calculate location of the particle in pixels;
        float cx = int(M.m10/M.m00);
        float cy = int(M.m01/M.m00);

//calculate current location from pixels to mm;
        float cx_mm = (cx-x_midpoint)/pixels;
        float cy_mm = (y_midpoint-cy)/pixels;
```

A.2 Magnetic field calculation using open-loop control

```
    float u_x_cap = TgtX_mm/k_cap; // With k_cap = 1/10.7
    float u_y_cap = TgtY_mm/k_cap; // Idem

    u_x += u_x_cap;
    u_y += u_y_cap;

// Calculate magnetic force output;
    float u = -sqrt(abs(u_x*u_x + u_y*u_y));
    float u_ang = atan2(u_y, u_x);
    float u_ang_deg = u_ang*180/M_PI;

    float B_mag = sqrt(abs(u));
    float B_ang = -0.5*u_ang;
    float B_ang_deg = B_ang*180/M_PI;

    resFieldX=B_mag*cos(B_ang);
    resFieldY=-B_mag*sin(B_ang);
```

A.3 PI controller

```
// difference;
    float error_x = TgtX_mm-cx_mm;
    float error_y = TgtY_mm-cy_mm;

// Integral part;
    iError_x += error_x * timestep;
    iError_y += error_y * timestep;

//PI Function;
    float u_x = Kp * error_x + Ki * iError_x;
    float u_y = Kp * error_y + Ki * iError_y;
```

A.4 Calculation of magnetic field from desired force

```
    float u = sqrt(abs(u_x*u_x + u_y*u_y));
    float u_ang = atan2(u_y, u_x);
    float u_ang_deg = u_ang*180/M_PI;

    float B_mag = sqrt(u);
    float B_ang = correct_angle(-0.5*u_ang);
    float B_ang_deg = B_ang*180/M_PI;
```

A.5 Mouseclick control

```
void Controller::CallBackFunc(int event, int x, int y, int flags, void* userdata)
{
    Controller* contr=(Controller*)userdata;

    if ( event == EVENT_LBUTTONDOWN )
    {
        contr->TgtX_mm = ((x-contr->x_midpoint)/contr->pixels);
        contr->TgtY_mm = ((contr->y_midpoint-y)/contr->pixels);
    }
}
```

```
setMouseCallback("Input frame", CallBackFunc, (void*)(this));
```